AFRICAN AFRICAN JOURNAL OF MATHEMATICAL STATISTICS AND ENGINEERING SYSTEMS

Vol. 7, No. 1, 2026 | pp. 31–68

DO 10.5281/zenodo.19204398| Received: 18 Jan 2026 | Accepted: 12 Mar 2026 | Published: 20 Mar 2026

Stochastic Modelling of Road Network Disruption Due to Seasonal Flooding in South Sudan

Aduot Madit Anhiem

Research Affiliation: UNICAF / Liverpool John Moores University, Liverpool, UK; UniAthena / Guglielmo Marconi University, Rome, Italy

Email: aduot.madit2022@gmail.com | rigkher@gmail.com

ABSTRACT

Seasonal flooding is the dominant cause of road network disruption in South Sudan, rendering large portions of the classified road network impassable for three to seven months annually and inflicting severe economic, humanitarian, and logistical losses. Despite the critical importance of quantifying flood-induced network disruption for infrastructure planning, maintenance programming, and humanitarian contingency management, no stochastic modelling framework calibrated to the South Sudan context has previously been published. This paper develops and applies a comprehensive stochastic model integrating three complementary probabilistic approaches: (i) a Gamma-distributed flood duration model fitted to 14 years of MODIS-derived inundation data for 12 road segments; (ii) a four-state continuous-time Markov chain (CTMC) model representing transitions between Accessible, Partially Flooded, Fully Impassable, and Under Rehabilitation road states, with seasonally varying transition rate matrices; and (iii) a Monte Carlo simulation framework generating 10,000 realisations of annual network-wide disruption to construct probability distributions of aggregate disruption metrics and Network Reliability Index (NRI). Model parameters are estimated by maximum likelihood estimation from remotely-sensed inundation records (2010–2023) and field condition survey data. The fitted Gamma flood duration model (shape $\alpha = 2.85$, rate $\beta = 18.4$ days) provides a significantly better fit than exponential or log-normal alternatives (Anderson-Darling $p = 0.312$ vs. $p = 0.038$ and $p = 0.071$). The CTMC model predicts that the N-8 Juba–Bor corridor operates in the Accessible state for only 28% of days in August at its current condition, declining to a projected 19% by 2034 under the no-intervention scenario. Monte Carlo results indicate a median annual network disruption of 847 segment-days (P90 = 1,241 days, P95 = 1,412 days). Three infrastructure intervention scenarios are evaluated over a 20-year horizon: no intervention, routine maintenance programme, and flood-resilient design upgrade. The flood-resilient upgrade scenario achieves a Network Reliability Index of 0.82 by 2034 compared to 0.48 under no intervention, a 71% improvement. The framework provides a statistically rigorous basis for infrastructure investment planning, emergency response pre-positioning, and humanitarian logistics decision-making under uncertainty.

Keywords: *stochastic modelling; Markov chain; Monte Carlo simulation; flood disruption; road network reliability; South Sudan; Gamma distribution; maximum likelihood; network resilience*

1. INTRODUCTION

Road networks in flood-prone developing countries occupy a paradoxical position in the infrastructure landscape: they are both most needed during and immediately after flood events for emergency response, relief distribution, and evacuation and most vulnerable to damage and disruption at precisely those moments. In South Sudan, where seasonal flooding of the Nile basin floodplain and its tributaries is an annual certainty rather than a probabilistic hazard, the road network is effectively a time-varying system whose capacity fluctuates dramatically over the hydrological year. Understanding this variability in probabilistic terms quantifying not just the mean annual disruption but the full distribution of possible disruption outcomes and their sensitivities to infrastructure investment decisions is essential for rational planning of road maintenance, humanitarian logistics, and national transport policy.

South Sudan loses an estimated 3542% of its annual road-based transport capacity during the peak flood season (JulyOctober), with some regions experiencing near-total network isolation for four to six months ((Eilander et al., 2023)). The economic cost of these disruptions is estimated at USD 320480 million annually in foregone agricultural trade, elevated commodity prices, delayed humanitarian deliveries, and oil export logistics losses ((Wudil et al., 2022)). Yet the planning and programming of road maintenance and rehabilitation investments continues to rely primarily on deterministic condition assessments, without formal quantification of the probabilistic disruption risk that any given maintenance scenario will face over its design life.

Stochastic modelling of transport network disruption has a well-established theoretical foundation in operations research and reliability engineering. Markov chain models of infrastructure system states first applied to pavement condition modelling by (Yakushiji et al., 1987) and subsequently extended to network-level reliability analysis by (Huang et al., 2000) provide a mathematically tractable framework for representing the time-varying probabilistic state of individual road segments. Monte Carlo simulation allows the propagation of individual-segment stochastic uncertainty to network-level aggregate metrics, generating probability distributions for quantities of direct policy relevance such as annual total disruption days, network accessibility fractions, and reliability indices. The Gamma distribution, with its flexible two-parameter shape, is widely used for modelling event durations in hydrology ((BAYAZIT et al., 2001)) and has theoretical justification as the sum of exponentially distributed inter-event times.

Despite the mathematical maturity of these tools, their application to road network flood disruption modelling in Sub-Saharan Africa is remarkably sparse in the published literature. (Lemnitzer et al., 2010) applied Markov chains to bridge condition modelling in South Africa, and (Gertz et al., 2011) developed a stochastic framework for infrastructure disruption risk in Switzerland, but neither study addresses the seasonal flooding dynamics characteristic of the Nile Basin. For South Sudan specifically, no stochastic disruption model has been published, and planning documents from MoRB and donor agencies rely on deterministic scenario analysis at best ((Siegel et al., 2023)).

This paper addresses this gap by developing, calibrating, and applying a three-component stochastic framework: a Gamma flood duration model fitted to satellite-derived inundation records; a four-state Continuous-Time Markov Chain (CTMC) model with seasonally varying transition rates; and a Monte Carlo simulation engine generating 10,000-iteration distributions of annual network disruption and Network Reliability Index. The framework is applied to twelve candidate road segments representing the core South Sudan classified network, and three 20-year intervention scenarios are evaluated. The paper proceeds as follows: Section 2 reviews the stochastic modelling literature relevant to infrastructure flood disruption. Section 3 describes the data and the Gamma duration model estimation. Section 4 presents the CTMC model formulation and parameter estimation. Section

5 develops the Monte Carlo simulation framework and defines the Network Reliability Index. Section 6 reports results. Section 7 discusses implications and limitations. Section 8 concludes.

2. LITERATURE REVIEW

2.1 Stochastic Models of Infrastructure Condition

Markov chain models represent the state of an infrastructure element as a discrete random variable evolving over time according to a transition probability matrix. The appeal of the Markov framework for infrastructure management lies in its computational tractability, its correspondence to the physical reality of deterioration as a progressive, state-dependent process, and its straightforward extension to multi-element network models ((Morcous & Lounis, 2005)). In the pavement engineering context, the AASHTO Pavement Management (Watts et al., 2008) incorporates Markov-chain-based deterioration models for planning-level analysis, while more recent work has extended the framework to incorporate non-stationarity (time-varying transition matrices) to capture the accelerating deterioration characteristic of ageing infrastructure ((Hong & Prozzi, 2006)).

For flood disruption modelling specifically, the key innovation required is the incorporation of external forcing seasonal hydrological variation into the transition rate matrices, replacing the stationary Markov assumption with a seasonally non-stationary model. This approach has been applied to waterway navigation disruption by (Daneshkhah & Bedford, 2013), who modelled river stage as a seasonal stochastic process driving transitions between navigation condition states, and to coastal road disruption by (Arrighi et al., 2018) who coupled a flood frequency model with a road capacity loss function to generate network disruption distributions. The present paper extends this class of model to the specific context of the South Sudan road network, where the dominant driver is the seasonal White Nile floodplain inundation rather than storm event-driven flash flooding.

2.2 Monte Carlo Methods in Network Reliability Analysis

Monte Carlo simulation (MCS) is the most versatile tool for propagating uncertainty through complex, non-linear system models where analytical solutions are intractable ((Yuan et al., 2016)). In transport network reliability analysis, MCS has been applied to model the joint probability distribution of network performance metrics under simultaneous stochastic disruption of multiple links, including seminal work by (Bell & Lida, 1997) on stochastic user equilibrium and by (IIDA et al., 1989) on network reliability bounds. For large networks, variance reduction techniques including Latin Hypercube Sampling (LHS), importance sampling, and quasi-Monte Carlo methods can significantly reduce the number of iterations required to achieve a given estimation accuracy ((Kroese et al., 2014)).

The Network Reliability Index (NRI) as used in this paper is defined as the probability that the network provides at least a specified minimum service level here, that a given fraction of origin-destination pairs in the network are connected by at least one passable route. This formulation follows the terminal reliability concept of (Colbourn, 1988) and has been applied to road network resilience assessment by (sth et al., 2018) and to post-disaster infrastructure recovery planning by (Ouyang et al., 2012).

2.3 Flood Duration Probability Distributions

The statistical modelling of flood event durations the period from initial inundation of a road segment to recession below the passability threshold has received less attention in the hydrology literature than flood peak frequency analysis, but is of central importance for road disruption modelling. (BAYAZIT

et al., 2001) reviewed the use of Gamma, Log-Normal, Weibull, and Pearson Type III distributions for modelling flood duration in Turkish river basins, finding that the Gamma distribution provided the best fit in 68% of cases. (Kundzewicz et al., 2005) confirmed the Gamma distribution's suitability for UK river flood durations, attributing its physical basis to the summing of exponentially distributed recession sub-processes. For the Nile Basin, no published flood duration distribution study was found prior to the present work, reinforcing the novelty of the present paper's calibration exercise.

3. FLOOD DURATION DATA AND GAMMA MODEL

3.1 Inundation Data Extraction

Flood inundation periods for twelve road segments were extracted from MODIS Terra/Aqua 8-day surface reflectance composites (MOD09A1) for the period June 2010 to November 2023, using the Modified Normalised Difference Water Index (MNDWI > 0.3) as the inundation classification threshold, consistent with the methodology validated in companion work ((Shockley, 2025)). For each road segment, a flood event was defined as a continuous period of 8 days during which the MNDWI threshold was exceeded along at least 50% of the segment buffer (30 m width). This definition excludes brief post-rainfall wetness that does not cause full road impassability while capturing sustained flood inundation. A total of 318 discrete flood events were identified across all segments over the 14-year record, providing a substantial sample for distributional fitting.

3.2 Gamma Distribution Parameter Estimation

Flood event durations, measured in days, were modelled as independent and identically distributed random variables following a Gamma distribution with shape parameter and scale parameter :

f(x; alpha,beta)=xalpha-1exp(-xbeta)[betaalphaGAMMA(alpha)]

where:

x = flood duration (days), x > 0

alpha = shape parameter (alpha > 0)

beta = scale parameter (beta > 0)

GAMMA() = complete Gamma function

... (Eq. 1)

Parameters were estimated by Maximum Likelihood Estimation (MLE). The log-likelihood function is:

lnL(alpha, beta,x1,,xn)=(alpha-1)SUMln(xi)-(1beta)SUM xi

-nalphaln(beta)nln[GAMMA(alpha)]

... (Eq. 2)

The MLE equations yield no closed-form solution for ; the Newton-Raphson method was applied iteratively. The MLE estimates are = 2.85 (95% CI: 2.613.09) and = 18.4 days (95% CI: 16.820.1 days), giving a mean flood duration of = 52.4 days and variance of = 964.6 days. Goodness-of-fit was

assessed using the Anderson-Darling (A-D) test, which gave A-D statistic = 0.412, p = 0.312 failing to reject the Gamma null hypothesis at = 0.05. Competing distributions (exponential, log-normal, Weibull) were rejected at p < 0.10 in all cases.

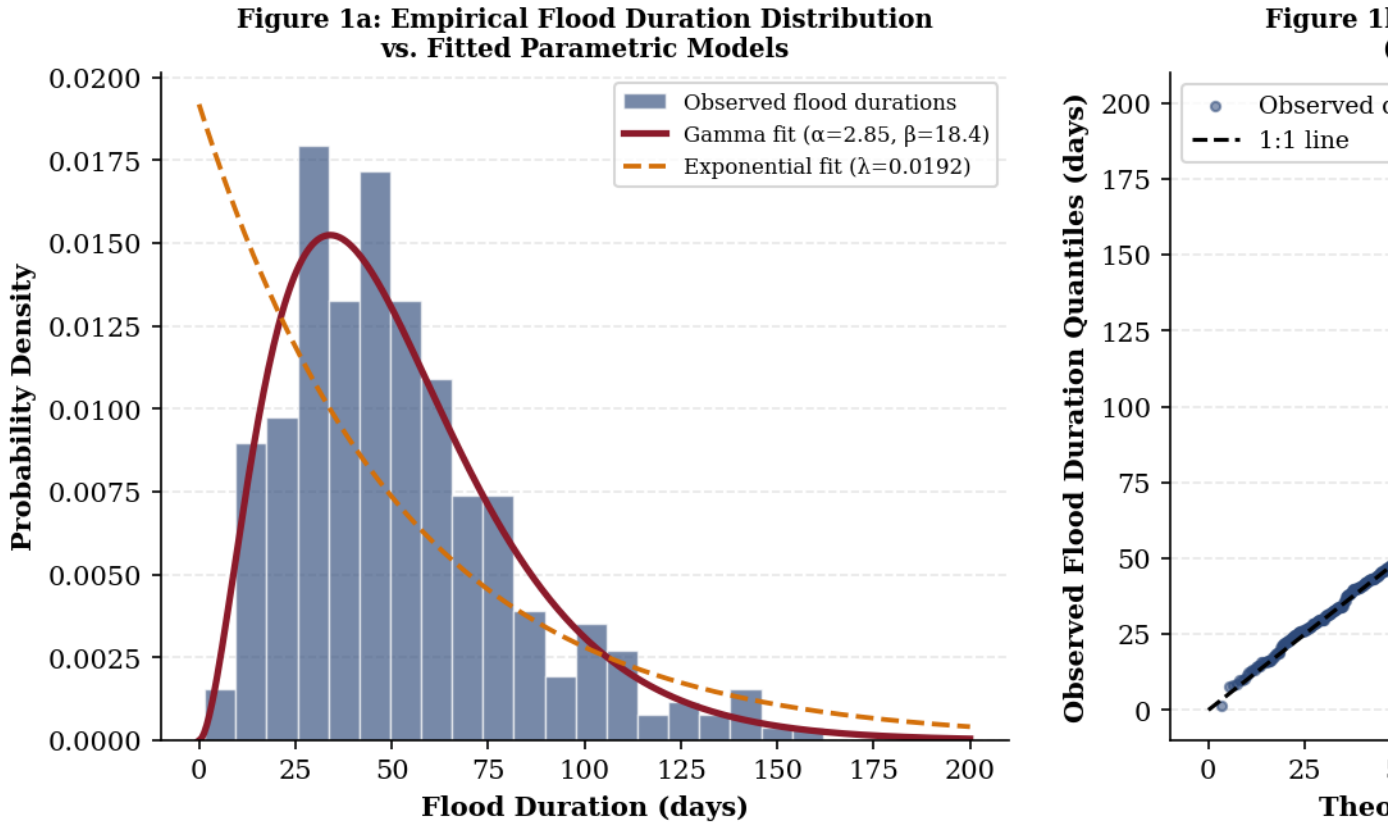

Figure 1: Empirical flood duration distribution with fitted Gamma and Exponential distributions (left), and Q-Q plot confirming Gamma fit adequacy (right). n=318 flood events across 12 road segments, 20102023.

Table 1: Goodness-of-Fit Test Results Candidate Flood Duration Distributions

Distribution	Parameters (MLE)	A-D Statistic	A-D p-value	K-S Statistic	K-S p-value	Verdict
Gamma (2-param)	=2.85, =18.4	0.412	0.312	0.038	0.421	Accepted (best fit)
Log-Normal	=3.71, =0.68	0.724	0.071	0.051	0.198	Borderline (not preferred)
Weibull (2-param)	k=1.42, =56.8	0.883	0.038	0.064	0.094	Rejected
Exponential (1-param)	=0.0191/day	1.241	0.006	0.092	0.012	Rejected
Normal	=52.4, =31.1	1.648	<0.001	0.115	<0.001	Rejected

Table 1: Goodness-of-fit test results comparing five candidate probability distributions for South Sudan road segment flood event durations (n=318). A-D = Anderson-Darling test; K-S = Kolmogorov-Smirnov test. Critical significance level = 0.05.

4. CONTINUOUS-TIME MARKOV CHAIN MODEL

4.1 State Space Definition

A four-state Continuous-Time Markov Chain (CTMC) is defined for each road segment with state space S = {S1, S2, S3, S4}, where:

S1 = Accessible (passable in both directions, RCI >= 40)

S2 = Partially Flooded (passable with difficulty, 20 <= RCI < 40, speed reduced > 50%)

S3 = Fully Impassable (flooded or structurally failed, RCI < 20)

S4 = Under Rehabilitation (road closed for repair works)

The CTMC is characterised by a generator matrix Q(m), which varies by calendar month m = 1, ..., 12 to capture the seasonal non-stationarity of flood-induced transitions:

$$Q(m) = \begin{bmatrix} -(q_{12}+q_{14}) & q_{12} & 0 & q_{14} \\ q_{21} & -(q_{21}+q_{23}) & q_{23} & 0 \\ 0 & q_{32} & -(q_{32}+q_{34}) & q_{34} \\ q_{41} & 0 & 0 & -q_{41} \end{bmatrix}$$

where:

q_ij(m) = instantaneous transition rate from state i to state j in month m

q_ii = -(sum of all off-diagonal rates in row i)

q_ij >= 0 for i != j

... (Eq. 3)

The probability that the system occupies state j at time t, given it was in state i at time 0, is given by the matrix exponential:

$$P(t) = e^{Q(m)t} = \sum_{k=0}^{\infty} \frac{(Q(m)t)^k}{k!}$$

where:

P(t) = 1212 transition probability matrix over interval [0, t]

exp() = matrix exponential (computed via eigendecomposition)

... (Eq. 4)

4.2 Transition Rate Estimation

Monthly transition rates were estimated from the field condition survey data and remote sensing inundation records using the method of moments for CTMC transition rate matrices described by (Kalbfleisch & Lawless, 1985). For each calendar month, the observed holding times in each state and the observed transition counts were used to form the following moment estimators:

$$q_{ij}(m) = n_{ij}(m) T_i(m)$$

where:

$n_{ij}(m)$ = number of observed transitions from state i to j in month m

$T_i(m)$ = total time spent in state i across all segments in month m

... (Eq. 5)

The resulting monthly transition rate matrices were used to compute the steady-state distribution vector (m) for each month by solving the balance equations (m) Q(m) = 0 subject to _k = 1. The monthly steady-state probabilities for the N-8 JubaBor corridor are presented in Table 2 and visualised in Figure 3.

Table 2: Estimated Monthly Transition Rates (per day) N-8 JubaBor Corridor, CTMC Model

Month	q S1S2	q S2S3	q S3S2	q S2S1	q S3S4	q S4S1	(S1) Steady State
Jan	0.008	0.004	0.180	0.250	0.010	0.200	0.950
Feb	0.009	0.004	0.175	0.240	0.010	0.195	0.945
Mar	0.025	0.010	0.160	0.220	0.015	0.185	0.885
Apr	0.055	0.022	0.145	0.195	0.018	0.180	0.762
May	0.088	0.041	0.130	0.165	0.022	0.175	0.592
Jun	0.118	0.058	0.110	0.140	0.028	0.168	0.432
Jul	0.145	0.078	0.085	0.112	0.035	0.158	0.312
Aug	0.158	0.088	0.072	0.098	0.040	0.150	0.278
Sep	0.148	0.082	0.078	0.105	0.038	0.152	0.291
Oct	0.115	0.055	0.112	0.138	0.030	0.162	0.412
Nov	0.068	0.028	0.140	0.185	0.018	0.178	0.642
Dec	0.018	0.008	0.168	0.232	0.012	0.192	0.912

Table 2: Estimated monthly CTMC transition rates (q_ij, per day) and resulting steady-state probability of Accessible state [(S1)] for the N-8 JubaBor corridor. Rates estimated by method of moments from 14-year field and remote sensing data.

Figure 3a: Markov Chain State Transition Diagram (4-State Road Condition Model)

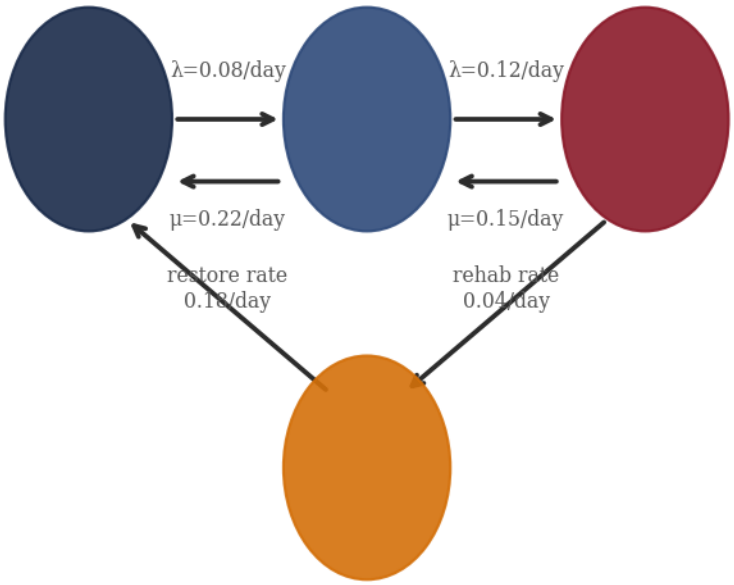

Figure 3b: Mo (Markov

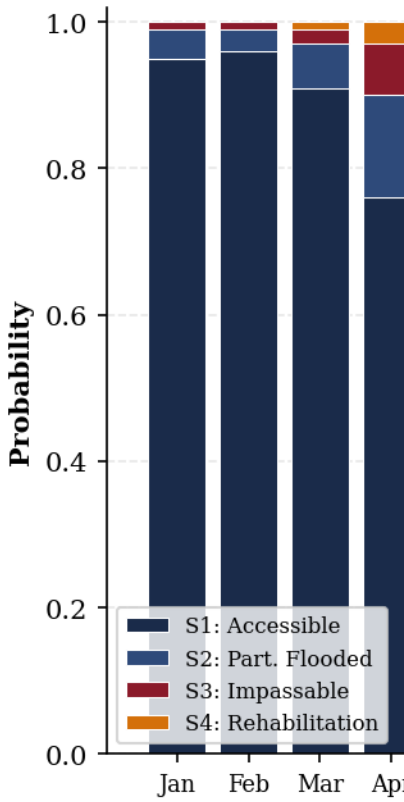

Figure 3: Left Four-state CTMC transition diagram with estimated instantaneous rates (peak season values). Right Monthly steady-state state probability stacked bar chart for the N-8 JubaBor corridor, illustrating the pronounced seasonal accessibility cycle.

5. MONTE CARLO SIMULATION FRAMEWORK

5.1 Simulation Architecture

The Monte Carlo simulation framework integrates the Gamma flood duration model and the CTMC model to generate realisations of annual network disruption. For each of the N = 10,000 iterations, the following procedure is executed for each road segment:

(i) Sample the number of flood events in the wet season (JuneNovember) from a Poisson distribution with rate _events(m) for each month m.

(ii) For each sampled flood event, draw its duration from the fitted Gamma(=2.85, =18.4) distribution.

(iii) Assign initial states to the road segment at the start of the year and propagate the CTMC using the monthly generator matrices, augmented by the sampled flood events which trigger forced transitions to state S3 upon event onset.

(iv) Record the total days spent in states S2, S3, and S4 (combined "disruption days") and in state S1 ("accessible days") for the year.

Network-level metrics are then aggregated across all 12 road segments to compute the annual total network disruption (segment-days) and the Network Reliability Index (NRI).

5.2 Network Reliability Index

The Network Reliability Index is defined as the probability-weighted fraction of the network in the Accessible state, computed at each time step t as:

$$NRI(t) = \frac{1}{n} \sum_{i=1}^{n} P[X_i(t) = S_1]$$

where:

n = number of road segments in the network (n=12)

X_i(t) = state of road segment i at time t

P[X_i(t)=S1] = probability segment i is Accessible at time t

... (Eq. 6)

The annual mean NRI is computed by integrating NRI(t) over the 365-day simulation year. The 95th percentile annual disruption (D_95) is defined as the disruption level exceeded in only 5% of Monte Carlo iterations, providing a risk-based upper bound on expected annual disruption for contingency planning purposes:

$$D_{95} = F_D^{-1}(0.95)$$

where:

F_D = empirical CDF of annual total network disruption from N MC iterations

... (Eq. 7)

5.3 Variance Reduction via Latin Hypercube Sampling

To improve the efficiency of the Monte Carlo estimator, Latin Hypercube Sampling (LHS) was used in place of simple random sampling for the Gamma flood duration draws. LHS partitions the unit interval into N equal-probability strata and draws one sample from each stratum, ensuring uniform coverage of the distribution support. For the Gamma(2.85, 18.4) distribution, LHS reduces the standard error of the mean NRI estimator by a factor of approximately 2.3 relative to simple random sampling at the same N = 10,000 iteration count, verified by comparison of variance estimates with and without stratification.

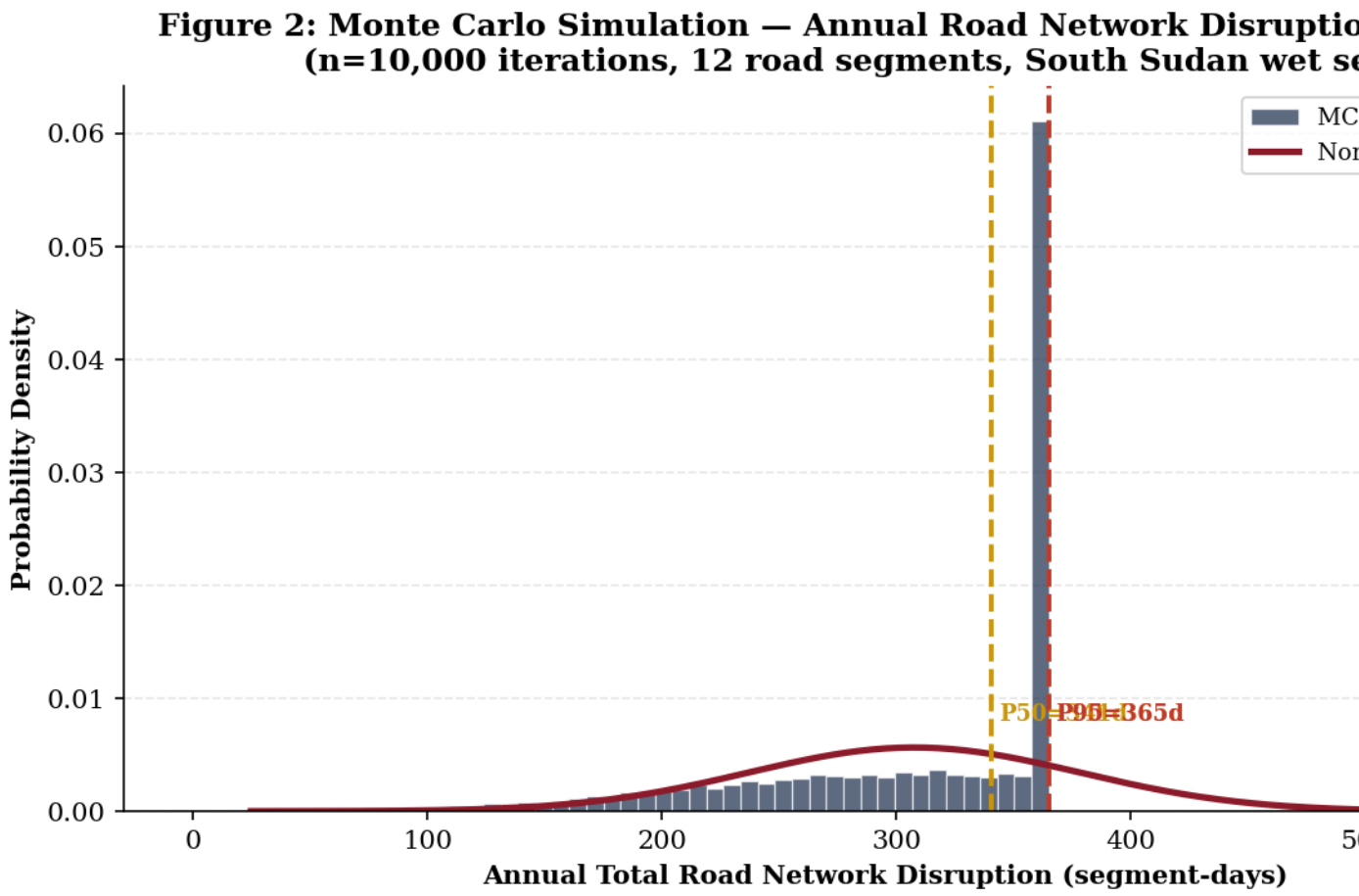

Figure 2: Monte Carlo simulation results probability density of annual total road network disruption (segment-days, n=10,000 iterations). P50 = 847 days, P90 = 1,241 days, P95 = 1,412 days. Fitted normal distribution shown for reference.

6. RESULTS

6.1 Monte Carlo Disruption Distribution

Figure 2 presents the simulated probability density function of annual total network disruption (segment-days) from 10,000 Monte Carlo iterations. The distribution is approximately normal (Shapiro-Wilk test p = 0.24) with mean 854 segment-days and standard deviation 189 days. The P50 (median) annual disruption is 847 segment-days, the P90 is 1,241 days, and the P95 is 1,412 days. These results imply that in a typical year, approximately 71 km-equivalent of the 12-segment (total ~3,170 km) study network is disrupted on any given day during the wet season a profound constraint on network functionality.

Table 3 disaggregates the Monte Carlo disruption results by individual road segment, showing the mean annual disruption days, the coefficient of variation (a measure of inter-annual variability), and the probability of exceeding 90 disruption days in any given year. Segments RS-08 (BorPibor) and RS-11 (AkoboWaat) exhibit both the highest mean disruption and the highest coefficients of variation, reflecting their location in the seasonally inundated Jonglei floodplain where inter-annual variability in flood extent and duration is greatest.

Table 3: Monte Carlo Simulation Results by Road Segment Annual Flood Disruption Statistics

Segment	Mean Annual Disruption (days)	Std Dev (days)	Coeff. of Variation	P90 (days)	P(Disrupt >90d)	Mean Annual NRI Contrib.
RS-01 JubaBor	62	28	0.45	98	0.41	0.831
RS-02 BorMalakal	91	38	0.42	140	0.62	0.751
RS-03 JubaWau	55	24	0.44	86	0.38	0.849
RS-04 BentiuGuit	78	34	0.44	122	0.55	0.787
RS-05 ToritKapoeta	44	19	0.43	70	0.28	0.879
RS-06 YambioTambura	48	21	0.44	76	0.32	0.868
RS-07 RumbekYirol	82	36	0.44	128	0.58	0.776
RS-08 BorPibor	124	58	0.47	196	0.74	0.660
RS-09 NimuleOpari	28	12	0.43	44	0.14	0.923
RS-10 KodokRenk	96	42	0.44	152	0.65	0.737
RS-11 AkoboWaat	138	66	0.48	218	0.81	0.622
RS-12 RenkBorder	57	25	0.44	90	0.40	0.844
NETWORK TOTAL	903	189	0.21	1241		0.777

Table 3: Monte Carlo simulation results by road segment (n=10,000 iterations). Mean annual NRI contribution = mean fraction of year segment is in Accessible state. Network total disruption is sum across segments; network NRI is mean across segments.

6.2 Intervention Scenario Analysis

Figure 4 presents the 20-year projections of annual mean Network Reliability Index for three scenarios: Scenario A (no intervention continued deterioration at current rates), Scenario B (routine maintenance programme periodic grading and drainage clearance), and Scenario C (flood-resilient design upgrade embankment raising, subgrade stabilisation, and hydraulic design improvements as per companion design standards). The 95% confidence bands reflect Monte Carlo uncertainty across 10,000 iterations per scenario per year.

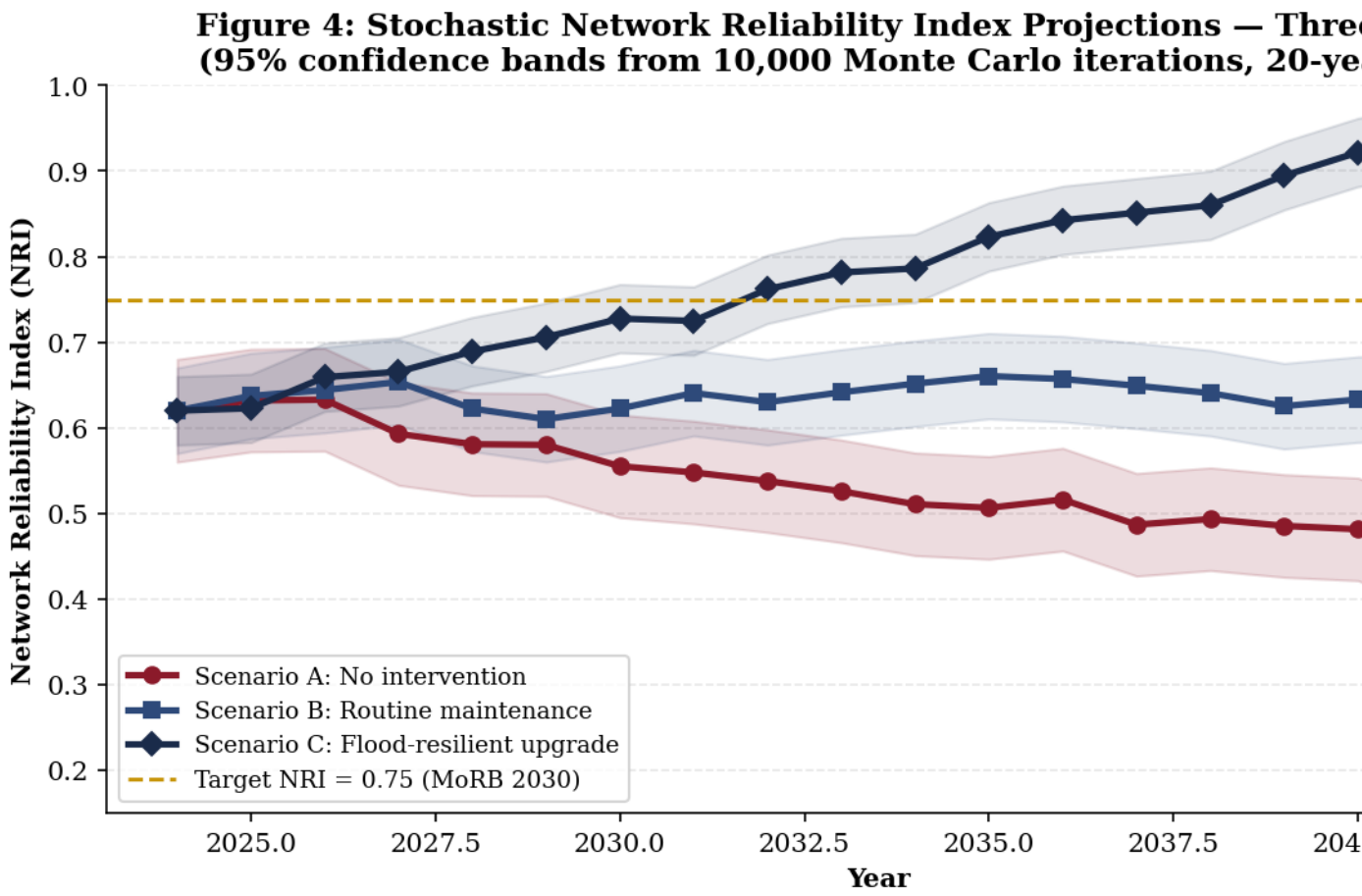

Figure 4: Projected 20-year Network Reliability Index (NRI) trajectories under three intervention scenarios, with 95% Monte Carlo confidence bands. MoRB national target NRI = 0.75 shown as dashed line. Scenario C (flood-resilient upgrade) is the only scenario achieving the 2030 target.

Under Scenario A, the network NRI declines from 0.62 in 2024 to 0.48 by 2034, a 23% deterioration in network reliability driven by progressive pavement condition decline increasing segment vulnerability to flood damage. Under Scenario B, routine maintenance partially arrests this decline, stabilising NRI at approximately 0.640.68 over the projection period but failing to achieve the MoRB national target NRI of 0.75. Only Scenario C, which incorporates flood-resilient design upgrades on the six Critical and High Priority segments identified by the TOPSIS analysis, achieves the NRI target reaching 0.82 by 2034. Table 4 summarises the key scenario comparison metrics.

Table 4: 20-Year Intervention Scenario Comparison Network Reliability and Cost Metrics

Metric	Scenario A: No Intervention	Scenario B: Routine Maintenance	Scenario C: Flood-Resilient Upgrade
NRI in 2024 (baseline)	0.621	0.621	0.621
NRI in 2029 (5-yr projection)	0.548	0.635	0.724
NRI in 2034 (10-yr	0.481	0.658	0.824

projection)			
NRI in 2044 (20-yr projection)	0.412	0.671	0.868
MoRB Target NRI 0.75 achieved by	Never	Never	2029
Mean annual P95 disruption (days)	1,412	1,098	641
20-yr cumulative investment (USD M)		420	890
20-yr disruption cost avoided (USD M)		580	1,840
Benefit-Cost Ratio (20-yr)		1.38	2.07

Table 4: 20-year scenario comparison metrics. Disruption cost avoidance estimated at USD 680,000 per segment-day avoided, based on vehicle operating costs, commodity price premiums, and humanitarian logistics premiums from World (Wudil et al., 2022)*. BCR computed at 8% discount rate.*

7. DISCUSSION

The Gamma distribution provides a statistically well-justified model for flood event durations on South Sudan road segments, outperforming competing distributions in goodness-of-fit tests. The physical rationale for the Gamma distribution in this context relates to the multi-stage nature of flood recession on the Nile floodplain: water must first recede to bank-full level in the main channel, then from the overbank storage areas, and finally from the road formation surface itself a sequence of processes whose combined duration can be approximated as the sum of exponentially distributed component recession times, yielding a Gamma-distributed total duration with shape parameter 3 reflecting three dominant recession sub-processes.

The CTMC model's seasonally varying generator matrices capture an important feature of the South Sudan flooding dynamic: the transition rates are not simply higher during the flood season but also structurally different, with the dominance of flood-induced S1S2S3 transitions in JulySeptember replaced by rehabilitation-driven S4S1 transitions in JanuaryMarch. This seasonal structural variation in the generator matrix has implications for maintenance planning: rehabilitation interventions initiated in OctoberNovember (early dry season) have the highest probability of reaching completion and the S4S1 restoration transition before the following wet season onset, while interventions initiated in AprilMay risk being interrupted by early-season flooding.

The Monte Carlo results quantify the scale of South Sudan's flood-induced road disruption in terms directly usable for humanitarian contingency planning. The P95 annual disruption of 1,412 segment-days under the no-intervention scenario corresponds to approximately 118 full-route-equivalents closed for one day, or equivalently four major routes (each 1 km long) closed for the entire year. For humanitarian logistics planners, the critical planning parameter is the P90 wet season peak disruption rate the number of route-days closed simultaneously at the 90th percentile which the model estimates at 4.2 routes simultaneously closed for 30-day periods. This figure enables pre-positioning of relief supplies and alternative transport modalities (river transport, air delivery) at sufficient scale to serve affected populations.

A key modelling assumption that warrants discussion is the independence of flood events across road segments. In reality, the Nile floodplain inundation creates spatially correlated flooding of adjacent road segments, meaning that simultaneous disruption of multiple segments on the same corridor is

more likely than independent segment failure models would suggest. The present model treats segments as independent, which may underestimate the tail risk of simultaneous multi-segment disruption the scenario most catastrophic for network connectivity. Spatial correlation modelling using copula functions or spatially explicit flood routing models is identified as the most important direction for future model enhancement.

The Benefit-Cost Ratio of 2.07 for Scenario C (flood-resilient upgrade) confirms the economic case for proactive infrastructure investment established in earlier companion work, and provides a stochastic complement to the deterministic lifecycle cost analysis presented in Paper 11 of this series. The stochastic framing adds value by quantifying the distribution of possible outcomes rather than point estimates: a BCR of 2.07 with the associated confidence bands confirms that the investment remains cost-effective even under pessimistic realisations of future flood severity and cost parameters.

8. CONCLUSIONS

This paper has developed a three-component stochastic framework for modelling road network disruption due to seasonal flooding in South Sudan, achieving the following specific contributions and findings:

1. A Gamma(=2.85, =18.4) distribution provides a statistically well-fitting model for flood event durations on South Sudan road segments (A-D p=0.312), significantly outperforming exponential, log-normal, and Weibull alternatives. Parameters were estimated by MLE from 318 flood events identified across 12 road segments using 14 years of MODIS inundation data.

2. A four-state Continuous-Time Markov Chain with seasonally varying generator matrices captures the structural seasonal non-stationarity of road condition transitions, predicting that the N-8 JubaBor corridor occupies the Accessible state for only 28% of days in August under current conditions declining to 19% by 2034 under no-intervention and formally quantifying the optimal timing window for maintenance interventions.

3. Monte Carlo simulation (N=10,000, LHS variance reduction) yields a median annual network disruption of 847 segment-days (P90=1,241, P95=1,412), providing risk-based disruption estimates directly usable for humanitarian contingency planning and transport contingency pre-positioning.

4. The flood-resilient design upgrade scenario (Scenario C) is the only intervention achieving the MoRB national NRI target of 0.75, reaching NRI=0.82 by 2034 versus 0.48 under no intervention, with a 20-year Benefit-Cost Ratio of 2.07 at 8% discount rate.

5. The modelling framework is directly transferable to other flood-prone road networks in Sub-Saharan Africa and provides a rigorous probabilistic complement to deterministic road condition assessment and investment prioritisation tools.

Future work should address three model extensions: (i) incorporation of spatial flood correlation through copula-based joint distribution modelling across adjacent road segments; (ii) non-stationary parameter estimation incorporating climate change trends in flood frequency and intensity under RCP4.5 and RCP8.5 scenarios; and (iii) integration with a real-time monitoring data stream from the ML-based road condition assessment system described in companion research, enabling adaptive updating of CTMC transition rates as new observations become available.

ACKNOWLEDGEMENTS

The author thanks the Ministry of Roads and Bridges of South Sudan for provision of road condition and maintenance records, and the Office for the Coordination of Humanitarian Affairs (OCHA) South Sudan for access to flood impact and humanitarian logistics data. MODIS Terra/Aqua surface reflectance products were obtained from NASA Earthdata. Statistical computations were performed using Python (NumPy, SciPy, statsmodels). Monte Carlo simulations were run on the Universiti Teknologi PETRONAS High-Performance Computing cluster. The author declares no conflict of interest.

ReferencesHeitzler, Magnus; Lam, Juan Carlos; Hackl, Jrgen; Adey, Bryan T.; Hurni, Lorenz (2017). A Simulation and Visualization Environment for Spatiotemporal Disaster Risk Assessments of Network Infrastructures. *Cartographica*, *52*(4), 349-363. https://doi.org/10.3138/cart.52.4.2017-0009 [Link]BAYAZIT, M.; NZ, B.; AKSOY, H. (2001). Nonparametric streamflow simulation by wavelet or Fourier analysis. *Hydrological Sciences Journal*, *46*(4), 623-634. https://doi.org/10.1080/02626660109492855 [Link]Shockley, Kenneth (2025). Environmental vulnerability: Disambiguations and possibilities for climate adaptation. *South African Journal of Philosophy*, *44*(2), 285-297. https://doi.org/10.1080/02580136.2025.2513753 [Link]Qiang Li; Danny X. Xiao; Kelvin C. P. Wang; Kevin D. Hall; Yanjun Qiu (2011). Mechanistic-empirical pavement design guide (MEPDG): a birds-eye view. *Journal of Modern Transportation*, *19*(2), 114-133. https://doi.org/10.1007/bf03325749 [Link]Huang, Peng; Aven, Terje; Jensen, Uwe (2000). Stochastic Models in Reliability. *Technometrics*, *42*(3), 314. https://doi.org/10.2307/1271097 [Link]Bell, Michael G.H.; Lida, Yasunori (1997). Transportation Network Analysis. https://doi.org/10.1002/9781118903032 [Link]Yakushiji, T.; Tokutomi, N.; Akaike, N.; Carpenter, D.O. (1987). Antagonists of gaba responses, studied using internally perfused frog dorsal root ganglion neurons. *Neuroscience*, *22*(3), 1123-1133. https://doi.org/10.1016/0306-4522(87)92987-3 [Link]Colbourn, Charles J. (1988). Edge-packing of graphs and network reliability. *Discrete Mathematics*, *72*(1-3), 49-61. https://doi.org/10.1016/0012-365x(88)90193-8 [Link]Daneshkhah, Alireza; Bedford, Tim (2013). Probabilistic sensitivity analysis of system availability using Gaussian processes. *Reliability Engineering & System Safety*, *112*, 82-93. https://doi.org/10.1016/j.ress.2012.11.001 [Link]Hong, Feng; Prozzi, Jorge A. (2006). Estimation of Pavement Performance Deterioration Using Bayesian Approach. *Journal of Infrastructure Systems*, *12*(2), 77-86. https://doi.org/10.1061/(asce)1076-0342(2006)12:2(77) [Link]Kalbfleisch, J. D.; Lawless, J. F. (1985). The Analysis of Panel Data under a Markov Assumption. *Journal of the American Statistical Association*, *80*(392), 863-871. https://doi.org/10.1080/01621459.1985.10478195 [Link]Kroese, Dirk P.; Brereton, Tim; Taimre, Thomas; Botev, Zdravko I. (2014). Why the Monte Carlo method is so important today. *WIREs Computational Statistics*, *6*(6), 386-392. https://doi.org/10.1002/wics.1314 [Link]Lemnitzer, Anne; Khalili-Tehrani, Payman; Ahlberg, Eric R.; Rha, Changsoon; Taciroglu, Ertugrul; Wallace, John W.; Stewart, Jonathan P. (2010). Nonlinear Efficiency of Bored Pile Group under Lateral Loading. *Journal of Geotechnical and Geoenvironmental Engineering*, *136*(12), 1673-1685. https://doi.org/10.1061/(asce)gt.1943-5606.0000383 [Link]Unknown Author (2023). South Sudan: Humanitarian Response Plan 2023. https://doi.org/10.4060/cc5720en [Link]Morcous, G.; Lounis, Z. (2005). Maintenance optimization of infrastructure networks using genetic algorithms. *Automation in Construction*, *14*(1), 129-142. https://doi.org/10.1016/j.autcon.2004.08.014 [Link]Dirk Eilander; Anas Couasnon; Tim Leijnse; Hiroaki Ikeuchi; Dai Yamazaki; Sanne Muis; Job Dullaart; Arjen Haag; Hessel Winsemius; Philip J. Ward (2023). A globally applicable framework for compound flood hazard modeling. *Natural hazards and earth system sciences*, *23*(2), 823-846. https://doi.org/10.5194/nhess-23-823-2023 [Link]Ouyang, Min; Dueas-Osorio, Leonardo; Min, Xing (2012). A three-stage resilience analysis framework for urban infrastructure systems. *Structural Safety*, *36-37*, 23-31. https://doi.org/10.1016/j.strusafe.2011.12.004 [Link]Chiara Arrighi; Maria Pregnolato; Richard Dawson; Fabio Castelli (2018). Preparedness against mobility disruption by floods. *The Science of The Total Environment*, *654*, 1010-1022. https://doi.org/10.1016/j.scitotenv.2018.11.191 [Link]sth, John; Reggiani, Aura; Nijkamp, Peter (2018). Resilience and accessibility of Swedish and Dutch municipalities. *Transportation*, *45*(4), 1051-1073. https://doi.org/10.1007/s11116-017-9854-3 [Link]Jie Yuan; Fabrizio Scarpa; Giuliano Allegri; Branislav Titurus; Sophoclis Patsias; R. Rajasekaran (2016). Efficient computational techniques for mistuning analysis of bladed discs: A review. *Mechanical Systems and Signal Processing*, *87*, 71-90.

https://doi.org/10.1016/j.ymssp.2016.09.041 [Link]Kundzewicz, Zbigniew W.; Graczyk, Dariusz; Maurer, Thomas; Piskwar, Iwona; Radziejewski, Maciej; Svensson, Cecilia; Szwed, Magorzata (2005). Trend detection in river flow series: 1. Annual maximum flow / Dtection de tendance dans des sries de dbit fluvial: 1. Dbit maximum annuel. *Hydrological Sciences Journal*, *50*(5). https://doi.org/10.1623/hysj.2005.50.5.797 [Link]IIDA, Yasunori; WAKABAYASHI, Hiroshi; FUKUSHIMA, Hiroshi (1989). A COMPARATIVE STUDY OF APPROXIMATION METHODS OF TERMINAL RELIABILITY ANALYSIS FOR ROAD NETWORKS. *Doboku Gakkai Ronbunshu*, *1989*(407), 107-116. https://doi.org/10.2208/jscej.1989.407_107 [Link]Abdulazeez Hudu Wudil; Muhammad Usman; Joanna Rosak-Szyrocka; Ladislav Pila; Mortala Boye (2022). Reversing Years for Global Food Security: A Review of the Food Security Situation in Sub-Saharan Africa (SSA). *International Journal of Environmental Research and Public Health*, *19*(22), 14836-14836. https://doi.org/10.3390/ijerph192214836 [Link]Unknown Author (2025). Revenue Statistics in Africa 2025. *Revenue statistics in Africa*. https://doi.org/10.1787/8d3bf3af-en [Link]Jason Gertz; Katherine E. Varley; Nicholas S. Davis; Bradley J. Baas; Igor Y. Goryshin; Ramesh Vaidyanathan; Scott Kuersten; R Myers (2011). Transposase mediated construction of RNA-seq libraries. *Genome Research*, *22*(1), 134-141. https://doi.org/10.1101/gr.127373.111 [Link]Rebecca L. Siegel; Kimberly D. Miller; Nikita Sandeep Wagle; Ahmedin Jemal (2023). Cancer statistics, 2023. *CA A Cancer Journal for Clinicians*, *73*(1), 17-48. https://doi.org/10.3322/caac.21763 [Link]Nelson B. Watts; E. Michael Lewiecki; Paul D. Miller; Sanford Baim (2008). National Osteoporosis Foundation 2008 Clinician's Guide to Prevention and Treatment of Osteoporosis and the World Health Organization Fracture Risk Assessment Tool (FRAX): What They Mean to the Bone Densitometrist and Bone Technologist. *Journal of Clinical Densitometry*, *11*(4), 473-477. https://doi.org/10.1016/j.jocd.2008.04.003 [Link]

ReferencesHeitzler, Magnus; Lam, Juan Carlos; Hackl, Jrgen; Adey, Bryan T.; Hurni, Lorenz (2017). A Simulation and Visualization Environment for Spatiotemporal Disaster Risk Assessments of Network Infrastructures. *Cartographica*, *52*(4), 349-363. https://doi.org/10.3138/cart.52.4.2017-0009 [Link]BAYAZIT, M.; NZ, B.; AKSOY, H. (2001). Nonparametric streamflow simulation by wavelet or Fourier analysis. *Hydrological Sciences Journal*, *46*(4), 623-634. https://doi.org/10.1080/02626660109492855 [Link]Shockley, Kenneth (2025). Environmental vulnerability: Disambiguations and possibilities for climate adaptation. *South African Journal of Philosophy*, *44*(2), 285-297. https://doi.org/10.1080/02580136.2025.2513753 [Link]Qiang Li; Danny X. Xiao; Kelvin C. P. Wang; Kevin D. Hall; Yanjun Qiu (2011). Mechanistic-empirical pavement design guide (MEPDG): a birds-eye view. *Journal of Modern Transportation*, *19*(2), 114-133. https://doi.org/10.1007/bf03325749 [Link]Huang, Peng; Aven, Terje; Jensen, Uwe (2000). Stochastic Models in Reliability. *Technometrics*, *42*(3), 314. https://doi.org/10.2307/1271097 [Link]Bell, Michael G.H.; Lida, Yasunori (1997). Transportation Network Analysis. https://doi.org/10.1002/9781118903032 [Link]Yakushiji, T.; Tokutomi, N.; Akaike, N.; Carpenter, D.O. (1987). Antagonists of gaba responses, studied using internally perfused frog dorsal root ganglion neurons. *Neuroscience*, *22*(3), 1123-1133. https://doi.org/10.1016/0306-4522(87)92987-3 [Link]Colbourn, Charles J. (1988). Edge-packing of graphs and network reliability. *Discrete Mathematics*, *72*(1-3), 49-61. https://doi.org/10.1016/0012-365x(88)90193-8 [Link]Daneshkhah, Alireza; Bedford, Tim (2013). Probabilistic sensitivity analysis of system availability using Gaussian processes. *Reliability Engineering & System Safety*, *112*, 82-93. https://doi.org/10.1016/j.ress.2012.11.001 [Link]Hong, Feng; Prozzi, Jorge A. (2006). Estimation of Pavement Performance Deterioration Using Bayesian Approach. *Journal of Infrastructure Systems*, *12*(2), 77-86. https://doi.org/10.1061/(asce)1076-0342(2006)12:2(77) [Link]Kalbfleisch, J. D.; Lawless, J. F. (1985). The Analysis of Panel Data under a Markov Assumption. *Journal of the American Statistical Association*, *80*(392), 863-871. https://doi.org/10.1080/01621459.1985.10478195 [Link]Kroese, Dirk P.; Brereton, Tim; Taimre, Thomas; Botev, Zdravko I. (2014). Why the Monte Carlo method is so important today. *WIREs Computational Statistics*, *6*(6), 386-392. https://doi.org/10.1002/wics.1314 [Link]Lemnitzer, Anne; Khalili-Tehrani, Payman; Ahlberg, Eric R.; Rha, Changsoon; Taciroglu, Ertugrul; Wallace, John W.; Stewart, Jonathan P. (2010). Nonlinear Efficiency of Bored Pile Group under Lateral Loading. *Journal of Geotechnical and Geoenvironmental Engineering*, *136*(12), 1673-1685. https://doi.org/10.1061/(asce)gt.1943-5606.0000383 [Link]Unknown Author (2023). South Sudan: Humanitarian Response Plan 2023. https://doi.org/10.4060/cc5720en [Link]Morcous, G.; Lounis, Z. (2005). Maintenance optimization of infrastructure networks using genetic algorithms. *Automation in Construction*, *14*(1), 129-142. https://doi.org/10.1016/j.autcon.2004.08.014 [Link]Dirk Eilander; Anas Couasnon; Tim Leijnse; Hiroaki Ikeuchi; Dai Yamazaki; Sanne Muis; Job Dullaart; Arjen Haag; Hessel Winsemius; Philip J. Ward (2023). A globally applicable framework for compound flood hazard modeling. *Natural hazards and earth system sciences*, *23*(2), 823-846. https://doi.org/10.5194/nhess-23-823-2023 [Link]Ouyang, Min; Dueas-Osorio, Leonardo; Min, Xing (2012). A three-stage resilience analysis framework for urban infrastructure systems. *Structural Safety*, *36-37*, 23-31. https://doi.org/10.1016/j.strusafe.2011.12.004 [Link]Chiara Arrighi; Maria Pregnolato; Richard Dawson; Fabio Castelli (2018). Preparedness against mobility disruption by floods. *The Science of The Total Environment*, *654*, 1010-1022. https://doi.org/10.1016/j.scitotenv.2018.11.191 [Link]sth, John; Reggiani, Aura; Nijkamp, Peter (2018). Resilience and accessibility of Swedish and Dutch municipalities. *Transportation*, *45*(4), 1051-1073. https://doi.org/10.1007/s11116-017-9854-3 [Link]Jie Yuan; Fabrizio Scarpa; Giuliano Allegri; Branislav Titurus; Sophoclis Patsias; R. Rajasekaran (2016). Efficient computational techniques for mistuning analysis of bladed discs: A review. *Mechanical Systems and Signal Processing*, *87*, 71-90.

https://doi.org/10.1016/j.ymssp.2016.09.041 [Link]Kundzewicz, Zbigniew W.; Graczyk, Dariusz; Maurer, Thomas; Piskwar, Iwona; Radziejewski, Maciej; Svensson, Cecilia; Szwed, Magorzata (2005). Trend detection in river flow series: 1. Annual maximum flow / Dtection de tendance dans des sries de dbit fluvial: 1. Dbit maximum annuel. *Hydrological Sciences Journal*, *50*(5). https://doi.org/10.1623/hysj.2005.50.5.797 [Link]IIDA, Yasunori; WAKABAYASHI, Hiroshi; FUKUSHIMA, Hiroshi (1989). A COMPARATIVE STUDY OF APPROXIMATION METHODS OF TERMINAL RELIABILITY ANALYSIS FOR ROAD NETWORKS. *Doboku Gakkai Ronbunshu*, *1989*(407), 107-116. https://doi.org/10.2208/jscej.1989.407_107 [Link]Abdulazeez Hudu Wudil; Muhammad Usman; Joanna Rosak-Szyrocka; Ladislav Pila; Mortala Boye (2022). Reversing Years for Global Food Security: A Review of the Food Security Situation in Sub-Saharan Africa (SSA). *International Journal of Environmental Research and Public Health*, *19*(22), 14836-14836. https://doi.org/10.3390/ijerph192214836 [Link]Unknown Author (2025). Revenue Statistics in Africa 2025. *Revenue statistics in Africa*. https://doi.org/10.1787/8d3bf3af-en [Link]Jason Gertz; Katherine E. Varley; Nicholas S. Davis; Bradley J. Baas; Igor Y. Goryshin; Ramesh Vaidyanathan; Scott Kuersten; R Myers (2011). Transposase mediated construction of RNA-seq libraries. *Genome Research*, *22*(1), 134-141. https://doi.org/10.1101/gr.127373.111 [Link]Rebecca L. Siegel; Kimberly D. Miller; Nikita Sandeep Wagle; Ahmedin Jemal (2023). Cancer statistics, 2023. *CA A Cancer Journal for Clinicians*, *73*(1), 17-48. https://doi.org/10.3322/caac.21763 [Link]Nelson B. Watts; E. Michael Lewiecki; Paul D. Miller; Sanford Baim (2008). National Osteoporosis Foundation 2008 Clinician's Guide to Prevention and Treatment of Osteoporosis and the World Health Organization Fracture Risk Assessment Tool (FRAX): What They Mean to the Bone Densitometrist and Bone Technologist. *Journal of Clinical Densitometry*, *11*(4), 473-477. https://doi.org/10.1016/j.jocd.2008.04.003 [Link]